Effect of high-pressure annealing on the normal-state transport of $LaO_{0.5}F_{0.5}BiS_2$

I. Pallecchi,* G. Lamura, and M. Putti
CNR-SPIN and Università di Genova, via Dodecaneso 33, I-16146 Genova, Italy

J. Kajitani, Y. Mizuguchi, and O. Miura
Department of Electrical and Electronic Engineering, Tokyo Metropolitan University, Hachioji, Tokyo 192-0397, Japan

S. Demura
Tokyo University of Science, 1-3 Kagurazaka, Shinjuku-ku, Tokyo 162-8601, Japan

K. Deguchi and Y. Takano
National Institute for Materials Science, Tsukuba, Ibaraki 305-0047, Japan
(Received 15 May 2014; revised manuscript received 12 June 2014; published 26 June 2014)

We study normal state electrical, thermoelectrical, and thermal transport in polycrystalline BiS_2-based compounds, which become superconducting by F doping on the O site. In particular, we explore undoped $LaOBiS_2$ and doped $LaO_{0.5}F_{0.5}BiS_2$ samples, prepared either with or without high-pressure annealing, in order to evidence the roles of doping and preparation conditions. The high-pressure annealed sample exhibits room temperature values of resistivity ρ around 5 mΩcm, Seebeck coefficient S around -20 μV/K, and thermal conductivity κ around 1.5 W/Km, while the Hall resistance R_H is negative at all temperatures and its value is -10^{-8} m^3/C at low temperature. The sample prepared at ambient pressure exhibits R_H positive in sign and five times larger in magnitude, and S negative in sign and slightly smaller in magnitude. These results reveal a complex multiband evolution brought about by high-pressure annealing. In particular, the sign inversion and magnitude suppression of R_H, indicating increased electron-type carrier density in the high-pressure sample, may be closely related to previous findings about change in lattice parameters and enhancement of superconducting T_c by high-pressure annealing. As for the undoped sample, it exhibits 10 times larger resistivity, 10 times larger $|S|$, and 10 times larger $|R_H|$ than its doped counterpart, consistent with its insulating nature. Our results point out the dramatic effect of preparation conditions in affecting charge carrier density as well as structural, band, and electronic parameters in these systems.

DOI: 10.1103/PhysRevB.89.214513 PACS number(s): 74.25.fc, 74.25.fg

I. INTRODUCTION

The crystal structure of layered superconductors, such as CuO_2-based and Fe-based compounds, is described as consisting of a charge reservoir layer plus a high mobility layer, with the former providing charge doping and the latter hosting the Cooper pairs. This charge transfer scenario has offered a key to understanding superconducting mechanisms in these materials and, even more importantly, it has driven the efforts of researchers towards the synthesis of new superconductors. Indeed, a new class of layered superconductors has been discovered very recently, namely BiS_2-based compounds such as $Bi_4O_4S_3$ ($T_c \sim 4.5$ K) [1,2], $Sr_{1-x}La_xFBiS_2$ [3], and $RO_{1-x}F_xBiS_2$ (R = La, Ce, Pr, Nd) systems. Among the latter ones, $LaO_{0.5}F_{0.5}BiS_2$ exhibits the largest onset $T_c \sim 11.1$ K [4,5]. The crystal structure of $La(O,F)BiS_2$ is composed of a stacking of $La_2(O,F)_2$ layers and double BiS_2 layers. In terms of electronic bands, the parent compound $LaOBiS_2$ is a band insulator with an energy gap of 0.4 eV between a valence band consisting of O and S p states and a conduction band consisting of Bi $6p$ and S $3p$ states [6]. With the partial substitution of O by F, electrons are doped into the conduction band and eventually superconductivity appears, with a maximum T_c of about 3 K for $x = 0.5$, in correspondence of a topological change of the Fermi surface [6,7]. More specifically, the Fermi surface is markedly two-dimensional and close to $x = 0.5$ it fulfills good nesting conditions [6,7]. From the calculation of the phonon spectrum and electron-phonon coupling constant for $LaO_{0.5}F_{0.5}BiS_2$ ($\lambda = 0.8$) [8], it turns out that this material is a conventional phonon mediated superconductor; however, it has been suggested that although the electron-phonon interaction plays the main role in the Cooper pairing, the good Fermi surface nesting may cooperate to give an enhanced attractive pairing interaction around the nesting vectors [7], by analogy with what is generally accepted to occur for iron-based superconductors. This gives rise to an s-wave pairing with a constant gap sign, which has been indeed observed experimentally by muon-spin spectroscopy [9]. Nevertheless, the issues of pairing mechanism and pairing symmetry are still under debate. Indeed, scanning tunneling microscopy studies have found very large values of the reduced gap in BiS_2 based superconductors [10], more compatible with unconventional pairing symmetry than with conventional s-wave superconductivity. Moreover, neutron scattering studies have suggested that the electron-phonon coupling in $LaO_{0.5}F_{0.5}BiS_2$ could be weaker than expected [11]. Additional investigation of the relationship between superconducting and normal state properties may add further clues about the phase diagram and thereby also about the conventional versus unconventional character of the relevant pairing mechanism.

In this paper, we specifically address the issue of how F doping and preparation conditions, in particular high-pressure (2 GPa) annealing, affect normal state properties and

*Corresponding author: ilaria.pallecchi@spin.cnr.it

superconducting T_c in $LaO_{1-x}F_xBiS_2$ bulk samples. Indeed, it has been found that high-pressure annealing yields a uniaxial lattice contraction along the c axis, as well as elongation of the a axis [4,12], which could be positively linked with the enhancement of superconducting T_c from 3 to 11 K [4,13]. Also the effectiveness of charge doping may be more or less directly affected by the preparation conditions. Theoretical investigations have indicated F doping as the most effective way to induce free charge carriers in BiS_2 planes, as compared to other possible chemical substitutions [14]. A charge transfer of about 0.26 e per unit formula to the BiS_2 planes in $x = 0.5$ F doped samples has been calculated [6]. On the other hand, F doping has been predicted to affect the band gap [15], making the relationship between nominal and effective doping less straightforward. From the experimental point of view, it has been evidenced that Bi deficiency may severely decrease the actual charge doping with respect to the nominal one [16].

In the following, we present magnetotransport, thermoelectrical transport, and thermal transport characterization of the normal state of $LaO_{1-x}F_xBiS_2$ bulk samples in order to gain insight into the electronic properties of this compound. In particular, we examine an undoped sample ($x = 0$), as well as two optimally doped ones ($x = 0.5$) prepared with or without high-pressure annealing, and compare their behaviors.

II. EXPERIMENTAL

Polycrystalline samples of $LaO_{0.5}F_{0.5}BiS_2$ are prepared by solid-state reaction using powders of La_2S_3 (99.9%), Bi_2O_3 (99.9%), BiF_3(99.9%), Bi_2S_3, and grains of Bi (99.99%). The Bi_2S_3 powder is prepared by reacting Bi (99.99%) and S (99.99%) grains at 500 °C in an evacuated quartz tube. The starting materials with a nominal composition of $LaO_{0.5}F_{0.5}BiS_2$ are mixed well, pressed into pellets, sealed into an evacuated quartz tube and heated at 700 °C for 10 hours. As an additional step, the obtained polycrystalline samples are annealed at 600 °C under a high pressure of 2 GPa for 1 hour using a cubic-anvil high-pressure synthesis apparatus.

Magnetotransport behavior is investigated by means of a Physical Property Measurement System (PPMS) by Quantum Design at temperatures from room temperatures down to 2 K and in magnetic fields up to 9 T. Hall coefficients (R_H) are determined by measuring the transverse resistivity at selected fixed temperatures, sweeping the field from −9 T to 9 T. Seebeck (S) effect and thermal conductivity are measured with the PPMS Thermal Transport Option in continuous scanning mode with a 0.3 K/min cooling rate.

III. RESULTS

In Fig. 1, the resistivity ρ curves of the undoped and doped samples prepared either by conventional solid-state reaction at ambient pressure ($LaO_{0.5}F_{0.5}BiS_2$-LP) or by high-pressure annealing ($LaO_{0.5}F_{0.5}BiS_2$-HP) are presented. All three samples exhibit semiconducting behavior in the whole temperature range of the normal state. The values of the room temperature resistivity are 28 mΩcm for the undoped sample and an order of magnitude smaller for the doped ones, namely 3.2 mΩcm for $LaO_{0.5}F_{0.5}BiS_2$-LP and 4.8 mΩcm for $LaO_{0.5}F_{0.5}BiS_2$-HP, all in fair agreement with previous reports

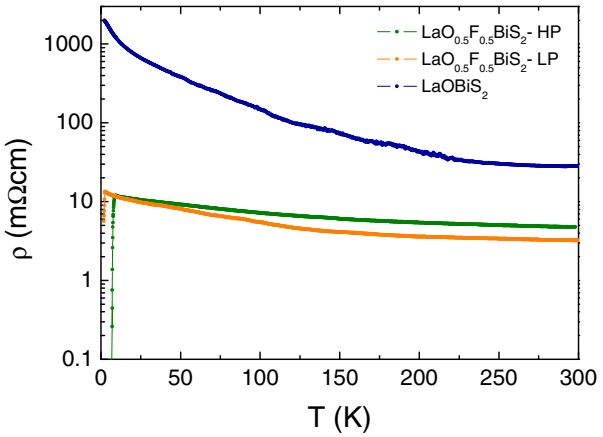

FIG. 1. (Color online) Resistivity versus temperature curves of undoped $LaOBiS_2$ and doped $LaO_{0.5}F_{0.5}BiS_2$ polycrystals, prepared either with or without high-pressure annealing.

[5,12,13,17]. Despite the two doped samples, $LaO_{0.5}F_{0.5}BiS_2$-LP and $LaO_{0.5}F_{0.5}BiS_2$-HP have similar resistivity values at low temperature, and the $LaO_{0.5}F_{0.5}BiS_2$-LP sample curve has a steeper temperature dependence, suggesting larger activation energy for transport. The doped sample $LaO_{0.5}F_{0.5}BiS_2$-LP becomes superconducting at temperature $T_{c-90\%} = 2.36$ K (defined at 90% of normal state resistivity), and the resistivity is not completely vanished at the minimum temperature of our measurement $T = 2$ K. In the case of the doped sample $LaO_{0.5}F_{0.5}BiS_2$-HP, we find a transition temperature $T_{c-90\%} = 8.46$ K and a transition width of 1.24 K. These data are again in agreement with previous works reporting on the effect of high-pressure annealing in improving superconducting properties [4,13].

The normal state longitudinal magnetoresistivity $[\rho(H) - \rho(H = 0)]/\rho(H = 0)$, not shown, is negligibly small (<1%) at all temperatures for all the samples.

In Fig. 2, Hall effect curves of the three samples are plotted. In the case of the doped $LaO_{0.5}F_{0.5}BiS_2$-HP sample, R_H is negative at all temperatures and slightly increasing in magnitude with decreasing temperature, with a value around -10^{-8} m^3/C

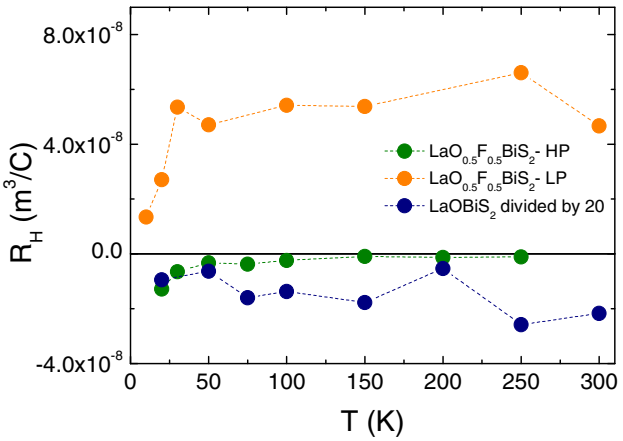

FIG. 2. (Color online) Hall coefficient versus temperature curves of undoped $LaOBiS_2$ and doped $LaO_{0.5}F_{0.5}BiS_2$ polycrystals, prepared either with or without high-pressure annealing.

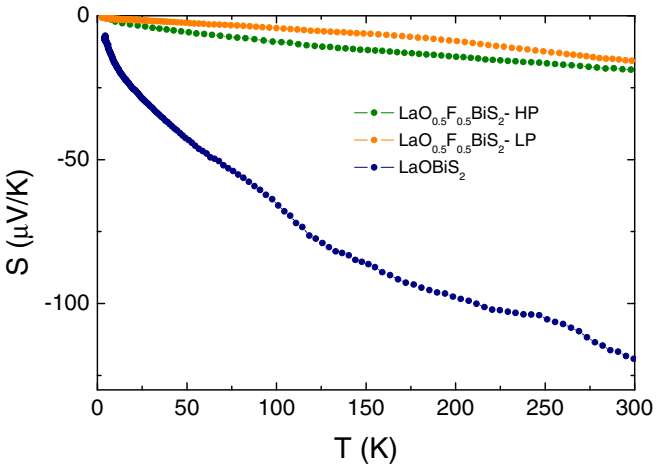

FIG. 3. (Color online) Seebeck effect coefficient versus temperature curves of undoped $LaOBiS_2$ and doped $LaO_{0.5}F_{0.5}BiS_2$ polycrystals, prepared either with or without high-pressure annealing.

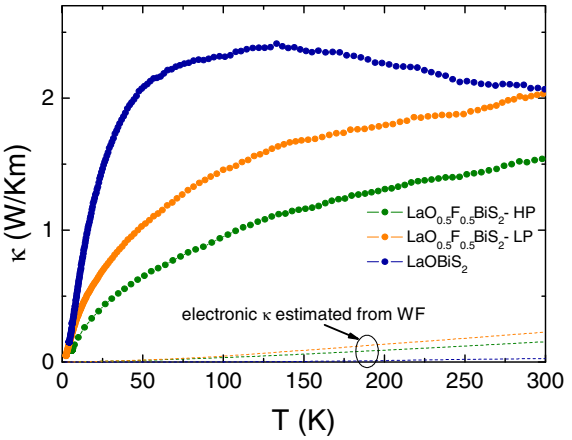

FIG. 4. (Color online) Thermal conductivity versus temperature curves of undoped $LaOBiS_2$ and doped $LaO_{0.5}F_{0.5}BiS_2$ polycrystals, prepared either with or without high-pressure annealing. Dashed lines indicate the electronic contribution to the thermal conductivity estimated with the Wiedemann-Franz (WF) law.

at low temperature just above the superconducting transition. This behavior is indeed reminiscent of that of Fe-based superconductors of different families, e.g., F doped 1111 compounds [18,19], electron-doped 122 compounds [20,21], and other families of Fe-based superconductors [22]. For the $LaO_{0.5}F_{0.5}BiS_2$-LP sample the magnitude of R_H is on average five times as much, consistent with other literature data [23], indicating lower electron density. However, quite remarkably, it is positive in sign. Positive R_H has also been found in other BiS_2 superconductors at optimal electron doping [24]. Finally, R_H of the $LaOBiS_2$ sample is negative, weakly dependent of temperature, and its magnitude is around a few times 10^{-7} m^3/C, i.e., 10 times larger than that of the corresponding doped $LaO_{0.5}F_{0.5}BiS_2$-LP sample.

It must be said that whereas for the $LaO_{0.5}F_{0.5}BiS_2$-HP sample Hall effect measurements are carried out easily, in the case of the $LaO_{0.5}F_{0.5}BiS_2$-LP and $LaOBiS_2$ samples the experimental data points are more scattered, not due to the magnitude of the Hall signal itself but possibly due to charging at grain boundaries. Also bismuth and bismuth oxide impurities may be responsible for erratic Hall effect measurements, but in our case bismuth phase is not detected by x-ray diffraction analysis; moreover, the negligible magnetoresistance is not consistent with magnetotransport behavior of bismuth and bismuth oxides.

In Fig. 3, we present Seebeck coefficient S curves of the three samples. It can be seen that in all cases, the Seebeck coefficients are roughly linear with temperature, suggesting that the diffusive mechanism of charge carriers dominates. This result is in agreement with similar optimally doped compounds such as $PrO_{0.3}F_{0.7}BiS_2$ [25] but at odds with other BiS_2-based superconductors, where nonmonotonic behavior with a pronounced minimum possibly related to a drag mechanism is observed [26]. Contrary to Hall resistance curves, the Seebeck coefficient curves are negative at all temperatures for all three samples. In particular, the $LaO_{0.5}F_{0.5}BiS_2$-LP exhibits negative S and positive R_H, similar to the case of other electron-doped BiS_2 superconductors [24]. No appreciable dependence on magnetic field is detected in the normal state Seebeck curves (in-field curves are not shown in Fig. 3), as expected in the diffusive regime. Only below T_c of the doped samples do the Seebeck curves at $\mu_0 H = 7$ T and 0 T deviate, as a consequence of the finite upper critical field.

In Fig. 4, thermal conductivity κ curves of the three samples are displayed. For the undoped sample, the thermal conductivity increases with temperature at low temperature, exhibits a maximum around $T = 100$ K, and levels off at higher temperatures. On the other hand, both the doped samples exhibit monotonic thermal conductivity and smaller thermal conductivity values. The doped $LaO_{0.5}F_{0.5}BiS_2$-HP sample has smaller thermal conductivity than the $LaO_{0.5}F_{0.5}BiS_2$-LP sample. No dependence of κ on magnetic field is observed (in-field curves are not shown in Fig. 4).

IV. DATA ANALYSIS AND DISCUSSION

Combining resistivity, Hall coefficient, and Seebeck coefficient data, we can carry out a fit of normal state properties, with carrier densities n, mobilities μ, and effective masses $m_{\rm eff}$ as parameters. In a single band picture we use for resistivity and the Hall coefficient, the relationships $\rho = (en\mu)^{-1}$ and $R_H = (en)^{-1}$, while for the Seebeck coefficient we use the Mott relationship valid for isotropic degenerate materials in the diffusive regime:

$$S = -\frac{\pi^2}{3}\left(\frac{k}{e}\right)kT\left(\frac{d\ln\sigma(E)}{dE}\right)\Bigg|_{E_F} \approx -\left(\frac{3}{2}+\alpha\right)\frac{8\pi^{8/3}k^2}{3^{5/3}h^2e}m_{\rm eff}\frac{T}{n}, \quad (1)$$

where k is the Boltzmann constant, h the Planck constant, E is the energy of charge carriers, α characterizes the energy dependence of the scattering time $\tau \sim E^{\alpha}$ (which is assumed constant for simplicity, i.e., $\alpha \sim 0$), σ is the conductivity ($\sigma = \rho^{-1}$), and the logarithmic derivative is calculated at the Fermi level. The minus sign holds for n-type charge carriers. To get the above expression in terms of fitting parameters n and $m_{\rm eff}$, a free electron picture with parabolic dispersion and

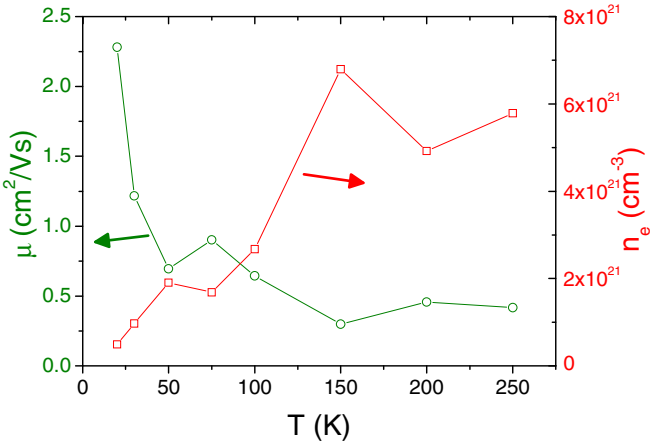

FIG. 5. (Color online) Electron charge density and mobility obtained from single band fitting of ρ and R_H data of the doped $LaO_{0.5}F_{0.5}BiS_2$-HP sample, prepared with high-pressure annealing.

spherical Fermi surface is assumed. In case of a two band picture, with electrons (subscript e) and holes (subscript h) contributing to transport, the appropriate relationships would be $\rho = ((en_e\mu_e)^{-1} + (en_h\mu_h)^{-1})^{-1}$, $R_H = \frac{1}{e}\frac{(\mu_h^2 n_h - \mu_e^2 n_e)}{(\mu_h n_h - \mu_e n_e)^2}$, and $S = \frac{\sigma_h S_h + \sigma_e S_e}{\sigma_h + \sigma_e}$, where the Seebeck coefficients of each band are calculated according to the Mott relationship [Eq. (1)].

Clearly in a *single band approximation* these parameters are univocally determined, whereas if we assume both electron and hole contributions the solutions are not any more univocal. In Fig. 5, we show the mobility and carrier concentration resulting from the single band fitting of the $LaO_{0.5}F_{0.5}BiS_2$-HP sample. The electron mobility is on average ~0.5–2 $cm^2/(Vs)$, slightly decreasing with increasing temperature. The electron density is in the range $5{\cdot}10^{20}$–$7{\cdot}10^{21}$ cm^{-3}, slightly increasing with increasing temperature. Of note, $2.3{\cdot}10^{21}$ cm^{-3} is just what is expected from the nominal $x = 0.5$ F doping. Moreover, in Ref. [6], it is predicted that $0.7 + 0.26 = 0.96$ electrons per unit cell are doped in the BiS_2 layers of $LaO_{0.5}F_{0.5}BiS_2$, corresponding to $4.4{\cdot}10^{21}$ cm^{-3}, in fair agreement with our data. However, these charge carriers seem not to be very mobile, as seen from low mobility values and from semiconducting behavior of resistivity, possibly as a consequence of strong interaction with boson fluctuations, as a consequence of many-body interactions [7], or as in relation with the predicted quasinested Fermi surface leading to the charge density wave instability [27]. From the fitting, values of the electron effective mass around m_0 (m_0 bare electron mass) are obtained, in agreement with Ref. [26].

If we assume a *two band description* with hole and electron contributions, all the physically realistic solutions for the set of parameters present some common features: (i) electron mobilities are larger than hole mobilities at all temperatures; (ii) at low temperature electron densities are around 10^{21} cm^{-3} or larger and hole densities are one order of magnitude smaller than electron density, while at high temperature hole and electron densities are similar; (iii) effective masses are of the order of m_0. This picture indicates that below 100 K, the system can be approximately described in a single band picture, taking into account only the electron contribution to transport.

For the doped $LaO_{0.5}F_{0.5}BiS_2$-LP sample, it is not possible to assume a single band description because it could not account for the different sign of R_H and S. On the contrary, in a two band description this situation may occur because, roughly speaking, band contributions are weighed by $n\mu^2$ in the expression for R_H, while they are weighed by μ in the expression for S. Hence, if we allow for a band of electrons with smaller density and higher mobility as compared to the band of holes, this situation may determine the negative sign for S even with a positive R_H. All the different solutions compatible with our experimental data present common robust characteristics, namely the following: (i) both electron and hole mobilities increase with increasing temperature; μ_e varies from a few $cm^2/(Vs)$ at low temperature to several tens of $cm^2/(Vs)$ at 300 K, while μ_h is one order of magnitude smaller; (ii) both electron and hole densities are weakly temperature dependent except for the lowest temperature; n_e is 1–$5{\cdot}10^{18}$ cm^{-3}, while n_h is 10^{19}–10^{20} cm^{-3}; (iii) both effective masses are around 0.5–1 m_0. In short, according to this picture there are more holes than electrons, but holes have much lower mobility. It may appear strange that the $LaO_{0.5}F_{0.5}BiS_2$-LP sample has lower $|S|$ and at the same time lower carrier concentrations as compared to the $LaO_{0.5}F_{0.5}BiS_2$-HP sample. Indeed, this is a multiband effect, explained by the more balanced competition between electron and hole-type carriers in the former sample.

Finally single band fittings for the undoped $LaOBiS_2$ sample yield average electron density a few times 10^{19} cm^{-3}, a factor of 10 smaller than that of the corresponding doped sample $LaO_{0.5}F_{0.5}BiS_2$-LP, mobilities values that increase with temperature from 0.2 to 15 $cm^2V^{-1}s^{-1}$ and effective masses around ~0.5 m_0. Obviously a two band scenario is possible as well.

In summary, the simple inspection of rough experimental data of resistivity, Seebeck coefficient, and R_H in $LaO_{0.5}F_{0.5}BiS_2$-LP and $LaO_{0.5}F_{0.5}BiS_2$-HP samples reveal that these two samples are significantly different. Indeed, R_H of the $LaO_{0.5}F_{0.5}BiS_2$-LP sample is positive and nearly five times larger in magnitude than R_H of the $LaO_{0.5}F_{0.5}BiS_2$-HP sample, which is negative. S of the two samples are both negative, but the S magnitude in the $LaO_{0.5}F_{0.5}BiS_2$-LP sample is slightly smaller than S of the $LaO_{0.5}F_{0.5}BiS_2$-HP sample. Finally, resistivities are comparable in magnitude, but the curve of the $LaO_{0.5}F_{0.5}BiS_2$-LP sample has steeper temperature dependence, indicating larger activation energy in the $LaO_{0.5}F_{0.5}BiS_2$-LP sample. As a further step, the data analysis, despite its simplifying assumptions, confirms that the preparation conditions have a strong effect on normal state properties. The average values of the parameters obtained from the fittings in the three samples are summarized in Table I for easy comparison. The major difference between $LaO_{0.5}F_{0.5}BiS_2$-LP and $LaO_{0.5}F_{0.5}BiS_2$-HP samples is the enhanced electron density in the latter, which is likely closely related to the enhancement of superconducting T_c from 3 to 11 K [4,13]. Moreover, these data suggest that the preparation conditions yield not only different charge carrier densities, but also different band and electronic parameters, such as larger effective mass and lower mobility in the $LaO_{0.5}F_{0.5}BiS_2$-HP sample as compared to the $LaO_{0.5}F_{0.5}BiS_2$-LP sample. Both

TABLE I. Parameters obtained by the fitting of ρ, R_H, and S curves.

	$LaO_{0.5}F_{0.5}BiS_2$-HP (single band fit)	$LaO_{0.5}F_{0.5}BiS_2$-LP (two band fit)	$LaOBiS_2$ (single band fit)
charge density (cm^{-3})	$5{\cdot}10^{20}$–$7{\cdot}10^{21}$	electrons: 1–$5{\cdot}10^{18}$ holes: $7{\cdot}10^{19}$–$1.6{\cdot}10^{20}$	1–$5{\cdot}10^{19}$
charge mobility ($cm^2V^{-1}s^{-1}$)	0.5–1	electrons: 10–100 holes: 3–25	0.2–15
effective mass	$\sim 1\ m_0$	0.5–1 m_0	$\sim 0.5\ m_0$

the larger effective mass and the lower mobility may be possibly related to stronger coupling with boson excitations, indeed enhanced coupling strength at optimal doping has been suggested for BiS_2-based superconductors in Ref. [24]. We note also that the analysis of superconducting properties has indicated different band and electronic parameters in samples prepared either with or without high-pressure annealing [28].

We now consider the thermal conductivities of the three samples. For the undoped sample, the thermal conductivity increases with temperature at low temperature due to increasing excitation of phonons. In this regime the dominant phonon scattering mechanism is by defects and grain boundaries. At high temperature, the thermal conductivity decreases with temperature due to enhanced phonon-phonon scattering, which is the dominant scattering mechanism in this regime. At intermediate temperature, there is a broad maximum as a consequence of the crossover between the aforementioned regimes. It is expected that with increasing disorder or grain boundary density, the regime of defect scattering extends up to larger temperatures, and eventually the broad maximum is damped, yielding a monotonic shape of the $\kappa(T)$ curve. This is indeed the case of the F doped samples, which show monotonic behavior typical of more disordered materials (or materials with higher density of grain boundaries) as compared to the undoped sample, which seems to have a more ordered crystal lattice (or larger grains).

It may appear unexpected that the doped sample prepared at high pressure has smaller thermal conductivity than the one prepared at low pressure, given that the former should have higher density and better intergrain connection. On the other hand, this finding is consistent x-ray analysis [4], which exhibits more broadened x-ray peaks after high-pressure annealing. The broader peaks in high-pressure annealed samples indicate the presence of disorder and inhomogeneity, which may be due to a competition of tetragonal and monoclinic phases in high-pressure samples [29]. Structural inhomogeneity in similar samples has been also detected from the analysis of magnetotransport data in the superconducting state, where the upper critical field parallel to BiS planes has been found to be anisotropic, indicating that these crystalline planes are distorted into a lower symmetry as compared to the tetragonal structure [28]. It can be noted also that electronic mobility, which is smaller in the $LaO_{0.5}F_{0.5}BiS_2$-HP sample (see Table I), may be affected by such disorder and inhomogeneity.

Using the Wiedemann-Franz law, we estimate that the thermal conductivity is dominated by phonon thermal transport for all the samples, as indicated by the dashed lines in Fig. 4. This finding is consistent with the low charge carrier mobility (in all samples κ is larger than 1.5 W/Km at room temperature, while the corresponding electron contribution is estimated smaller than 0.2 W/Km). The absence of magnetic field dependence of κ is consistent, with κ being dominated by the lattice contribution.

V. CONCLUSIONS

We study normal state electrical, thermoelectrical, and thermal transport in polycrystalline undoped $LaOBiS_2$ and doped $LaO_{0.5}F_{0.5}BiS_2$ samples, prepared either by conventional solid-state reaction at ambient pressure or by additional high-pressure annealing.

All of our samples present common behaviors such as semiconducting resisitivity, diffusive and negative Seebeck effect, and thermal transport dominated by phonon contribution. However, the major difference between doped $LaO_{0.5}F_{0.5}BiS_2$ samples, prepared either by conventional solid-state reaction at ambient pressure or by high-pressure annealing, lies in the sign and magnitude of the Hall resistance, which is positive in sign and larger in magnitude in the former sample and negative in sign and smaller in magnitude in the latter sample. This finding indicates the role played by the multiband character of these compounds. The higher electron concentration of samples prepared by high-pressure annealing may be closely related to the enhanced superconducting $T_c \sim 11$ K and to the change of structural parameters. Our results indicate that not only charge carrier densities but also band and electronic parameters are affected by preparation conditions. This work should trigger *ab initio* calculations, which could provide a theoretical framework for our experimental outcomes.

ACKNOWLEDGEMENT

The work was supported by the FP7 European Project SUPER-IRON (Contract No. 283204).

[1] Y. Mizuguchi, H. Fujihisa, Y. Gotoh, K. Suzuki, H. Usui, K. Kuroki, S. Demura, Y. Takano, H. Izawa, and O. Miura, Phys. Rev. B **86**, 220510(R) (2012).

[2] S. K. Singh, A. Kumar, B. Gahtori, S. Kirtan, G. Sharma, S. Patnaik, and V. P. S. Awana, J. Am. Chem. Soc. **134**, 16504 (2012).

[3] X. Lin, X. Ni, B. Chen, X. Xu, X. Yang, J. Dai, Y. Li, X. Yang, Y. Luo, Q. Tao, G. Cao, and Z. Xu, Phys. Rev. B **87**, 020504 (2013).
[4] Y. Mizuguchi, T. Hiroi, J. Kajitani, H. Takatsu, H. Kadowaki, and O. Miura, J. Phys. Soc. Jpn. **83**, 053704 (2014).
[5] Y. Mizuguchi, S. Demura, Y. Takano, H. Fujihisa, Y. Gotoh, H. Izawa, and O. Miura, J. Phys. Soc. Jpn. **81**, 114725 (2012).
[6] I. R. Shein and A. L. Ivanovskii, JETP Lett. **96**, 769 (2012).
[7] H. Usui, K. Suzuki, and K. Kuroki, Phys. Rev. B **86**, 220501(R) (2012).
[8] B. Li, Z. W. Xing, and G. Q. Huang, arXiv:1210.1743 (2012).
[9] G. Lamura, T. Shiroka, P. Bonfa, S. Sanna, R. De Renzi, C. Baines, H. Luetkens, J. Kajitani, Y. Mizuguchi, O. Miura, K. Deguchi, S. Demura, Y. Takano, and M. Putti, Phys. Rev. B **88**, 180509(R) (2013).
[10] S. Li, H. Yang, D. L. Fang, Z. Y. Wang, J. Tao, X. X. Ding, and H.-H. Wen, Sci. China-Phys. Mech. Astron. **56**, 2019 (2013).
[11] J. Lee, M. B. Stone, A. Huq, T. Yildirim, G. Ehlers, Y. Mizuguchi, O. Miura, Y. Takano, K. Deguchi, S. Demura, and S.-H. Lee, Phys. Rev. B **87**, 205134 (2013).
[12] J. Kajitani, K. Deguchi, A. Omachi, T. Hiroi, Y. Takano, H. Takatsu, H. Kadowaki, O. Miura, and Y. Mizuguchi, Solid State Commun. **181**, 1 (2014).
[13] K. Deguchi, Y. Mizuguchi, S. Demura, H. Hara, T. Watanabe, S. J. Denholme, M. Fujioka, H. Okazaki, T. Ozaki, H. Takeya, T. Yamaguchi, O. Miura, and Y. Takano, Europhys. Lett. **101**, 17004 (2013).
[14] C. Morice, E. Artacho, S. E. Dutton, D. Molnar, H.-J. Kim, and S. S. Saxena, arXiv:1312.2615 (2013).
[15] K. Suzuki, H. Usui, and K. Kuroki, Physics Procedia **45**, 21 (2013).
[16] Z. R. Ye, H. F. Yang, D. W. Shen, J. Jiang, X. H. Niu, D. L. Feng, Y. P. Du, X. G. Wan, J. Z. Liu, X. Y. Zhu, H. H. Wen, and M. H. Jiang, arXiv:1402.2860 (2014).
[17] Y. Mizuguchi, arXiv:1311.4270 (2013).
[18] M. Tropeano, I. Pallecchi, M. R. Cimberle, C. Ferdeghini, G. Lamura, M. Vignolo, A. Martinelli, A. Palenzona, and M. Putti, Supercond. Sci. Technol. **23**, 054001 (2010).
[19] J. Jaroszynski, S. C. Riggs, F. Hunte, A. Gurevich, D. C. Larbalestier, G. S. Boebinger, F. F. Balakirev, A. Migliori, Z. A. Ren, W. Lu, J. Yang, X. L. Shen, X. L. Dong, Z. X. Zhao, R. Jin, A. S. Sefat, M. A. McGuire, B. C. Sales, D. K. Christen, and D. Mandrus, Phys. Rev. B **78**, 064511 (2008).
[20] F. Rullier-Albenque, D. Colson, A. Forget, P. Thuéry, and S. Poissonnet, Phys. Rev. B **81**, 224503 (2010).
[21] F. Rullier-Albenque, D. Colson, A. Forget, and H. Alloul, Phys. Rev. Lett. **103**, 057001 (2009).
[22] J. Guo, S. Jin, G. Wang, S. Wang, K. Zhu, T. Zhou, M. He, and X. Chen, Phys. Rev. B **82**, 180520(R) (2010).
[23] V. P. S. Awana, A. Kumar, R. Jha, S. K. Singh, A. Pal, Shruti, J. Saha, and S. Patnaik, Solid State Commun. **157**, 21 (2013).
[24] H. Sakai, D. Kotajima, K. Saito, H. Wadati, Y. Wakisaka, M. Mizumaki, K. Nitta, Y. Tokura, and S. Ishiwata, J. Phys. Soc. Jpn. **83**, 014709 (2014).
[25] R. Jha, H. Kishan, and V. P. S. Awana, J. Appl. Phys. **115**, 013902 (2014).
[26] P. Srivatsava, Shruti, and S. Patnaik, Supercond. Sci. Technol. **27**, 055001 (2014).
[27] X. G. Wan, H. C. Ding, S. Y. Savrasov, and C. G. Duan, Phys. Rev. B **87**, 115124 (2013).
[28] Y. Mizuguchi, A. Miyake, K. Akiba, M. Tokunaga, J. Kajitani, and O. Miura, Phys. Rev. B **89**, 174515 (2014).
[29] T. Tomita, M. Ebata, H. Soeda, H. Takahashi, H. Fujihisa, Y. Gotoh, Y. Mizuguchi, H. Izawa, O. Miura, S. Demura, K. Deguchi, and Y. Takano, J. Phys. Soc. Jpn. **83**, 063704 (2014).